

Supporting Information

Ultrathin Free-standing Nanosheets of Bi₂O₂Se: Room Temperature Ferroelectricity in Self-assembled Charged Layered Heterostructure

Tanmoy Ghosh,[†] Manisha Samanta,[†] Aastha Vasdev,[‡] Kapildeb Dolui,[§] Jay Ghatak^{||}, Tanmoy Das,[⊥] Goutam Sheet,^{‡,*} and Kanishka Biswas^{†,||,#,*}

[†]*New Chemistry Unit, Jawaharlal Nehru Centre for Advanced Scientific Research (JNCASR), Jakkur P.O., Bangalore 560064, India*

[‡]*Department of Physical Sciences, Indian Institute of Science Education and Research Mohali, Sector 81, S. A. S. Nagar, Manauli, P.O. Box 140306, India*

[§]*Department of Physics and Astronomy, University of Delaware, Newark, DE 19716-2570, USA*

^{||}*International Centre for Materials Science, Jawaharlal Nehru Centre for Advanced Scientific Research (JNCASR), Jakkur P.O., Bangalore 560064, India*

[⊥]*Department of Physics, Indian Institute of Science, Bangalore 560012, India*

[#]*School of Advanced Materials, Jawaharlal Nehru Centre for Advanced Scientific Research (JNCASR), Jakkur P.O., Bangalore 560064, India*

**E-mail: kanishka@jncasr.ac.in (K.B.); goutam@iisermohali.ac.in (G.S.)*

Methods

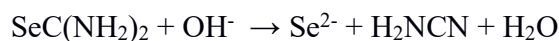
Reagents. Bismuth nitrate ($\text{Bi}(\text{NO}_3)_3 \cdot 5\text{H}_2\text{O}$, Alfa Aesar, 99.9%), selenourea ($\text{SeC}(\text{NH}_2)_2$, Alfa Aesar, 99.9%), potassium hydroxide (KOH, S D Fine-Chem Limited (SDFCL)), sodium hydroxide (NaOH, SDFCL), Disodium EDTA ($\text{C}_{10}\text{H}_{14}\text{O}_8\text{Na}_2\text{N}_2 \cdot \text{H}_2\text{O}$, SDFCL) and ethanol were used without any further purification.

Synthesis procedure. 100 mg (0.206 mmol) of $\text{Bi}(\text{NO}_3)_3 \cdot 5\text{H}_2\text{O}$, 12.7 mg (0.103 mmol) of $\text{SeC}(\text{NH}_2)_2$ and 306.8 mg (0.824 mmol) of disodium EDTA were sequentially added at a 5 minutes interval into 20 ml water in a glass beaker. The solution was stirred continuously. The addition of $\text{Bi}(\text{NO}_3)_3 \cdot 5\text{H}_2\text{O}$ into water results in a milky white color solution which turns into an orange color solution after the addition of $\text{SeC}(\text{NH}_2)_2$. The solution becomes clear after the addition of disodium EDTA. Finally, 120 mg (2.14 mmol) of KOH and 320 mg (8 mmol) of NaOH were added into the solution which turns the solution color black. After 10 minutes of stirring, the solution was put to rest which results in precipitation of the dark brown color nanosheets. We observed that nanosheets of similar morphology and thickness can also be obtained without using disodium EDTA, however, in that case, the required amount of water solvent is much higher, 200 ml. These were then washed with alcohol and water and centrifuged to remove disodium EDTA. The purified product was then dried in a vacuum oven at 150 °C.

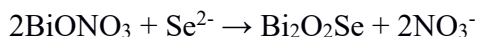
Step I: In water, $\text{Bi}(\text{NO}_3)_3$ undergoes hydrolysis to produce BiONO_3 and the process of hydrolysis is expedited in alkaline medium:



Step II: Selenourea $\text{SeC}(\text{NH}_2)_2$ undergoes decomposition in alkaline medium to generate selenide ions (Se^{2-}) along with cyanamide (H_2NCN):



Step III: In the final step, Se^{2-} interacts with BiONO_3 to form $\text{Bi}_2\text{O}_2\text{Se}$ which is precipitated as dark brown color product in the aqueous medium.



X-ray diffraction (XRD). Powder XRD patterns were collected in a Panalytical diffractometer with $\text{Cu K}\alpha$ radiation ($\lambda = 1.5406 \text{ \AA}$) at room temperature. XRD data of the as synthesized nanosheets were collected after dispersing the nanosheets in ethanol and drop casting on to a glass slide.

Band gap measurement. Diffuse reflectance spectroscopy was carried out using a Perkin Elmer Lambda 900, UV/VIS/NIR spectrometer from which absorption data was calculated using Kubelka-Munk equation: $\alpha/S = (1 - R)^2/2R$ where α , S and R are the absorption coefficient, scattering coefficient and reflectance, respectively. The optical band gap was then determined from the energy variation of α/S .

X-ray photoelectron spectroscopy (XPS). XPS measurement was carried out using an Omicron nanotechnology spectrometer with an $\text{Mg-K}\alpha$ (1253.6 eV) x-ray source.

Field emission scanning electron microscopy (FESEM). FESEM imaging was carried out using a FEI NOVA NANO SEM 600 with operating energy of 15 kV. Energy dispersive spectroscopy (EDX) analysis was carried out with an attached EDX genesis instrument.

Transmission electron microscopy (TEM). TEM studies were carried out using a FEI TECNAI G² 20 STWIN TEM operated at 200 keV and an aberration corrected FEI TITAN3 operating at 300 keV. EDX compositional analysis and elemental mapping were carried in STEM imaging mode. Very dilute solution of $\text{Bi}_2\text{O}_2\text{Se}$ nanosheets dispersed in ethanol was drop casted on holey carbon coated Cu grid and used for the TEM studies.

Inductively coupled plasma atomic emission spectroscopy (ICP-AES). ICP-AES was carried out for compositional analysis in a Perkin-Elmer Optima 7000DV instrument. For ICP-AES study, powdered nanosheets were dissolved in aqua regia ($\text{HNO}_3:\text{HCL} = 3:1$) and then this solution was further diluted using Millipore water.

Atomic force microscopy (AFM). Bruker Innova microscope in tapping mode was used to carry out AFM studies using an antimony doped silicon tip.

Raman Spectra. Room temperature Raman spectra of $\text{Bi}_2\text{O}_2\text{Se}$ bulk and nanosheet samples were collected on a Horiba Jobin Yvon LabRAM HR800 spectrometer using a He-Ne laser (632.8 nm).

Differential Scanning Calorimetry (DSC): A METTLER-TOLEDO differential scanning calorimeter (DSC 822 e) was used to collect DSC data with a ramp rate of 1 K/min in N_2 atmosphere.

Piezoresponse force microscopy (PFM). The measurements were done using an Asylum research AFM (MFP-3D) with an additional high voltage amplifier. The sample was mounted on a conducting sample holder which was directly connected to the ground of the amplifier. The conductive AFM cantilever having a Pt-Ir tip on it was brought in contact with the sample (nanosheets). An AC excitation of 4V riding on a dc bias voltage (V_{dc}) was applied between the tip and the amplifier ground. The response of the sample to the electrical stimulus was detected through the reflection of the laser beam from the end of the cantilever onto a position sensitive photo diode. In order to ensure that the hysteretic effects are due to ferroelectricity which may otherwise arise from electrostatic and electrochemical effect, all the measurements were performed following SS-PFM (switching spectroscopy piezoresponse force microscopy) initiated by Jesse et al.^{1,2} In this method, instead of sweeping V_{dc} continuously, bias is applied in sequence of pulses where the phase and amplitude measurements are done in the “off” states and an appreciable

change is observed in the “off-state” results as compared to the “on-state” measurements which is a clear evidence of the minimization of electrostatic effects. We further performed the topographic imaging after the spectroscopic measurements, where no topographic modification was observed which usually occurs due to the electrochemical reaction between the tip and sample.

Dielectric measurements. For dielectric measurements, Bi₂O₂Se nanosheets were pressed into a pellet. Dielectric properties were then measured in the temperature range from room temperature to 573 K and in the frequency range 200 Hz to 1 MHz with an ac excitation of 20 mV using a Solartron 1296A impedance analyzer.

Density functional theory (DFT) calculations. The first principles electronic structure calculations are performed within the framework of density functional theory (DFT) using generalized gradient approximation (GGA) of the Perdew-Burke-Ernzerhof (PBE)³ form for the exchange-correlation functional as implemented in the Vinea Ab-initio Simulation Package (VASP).⁴ The projector augmented wave (PAW)⁵ pseudo-potentials are used to describe the core electrons. Electronic wave-functions are expanded using plane waves up to a cut-off energy of 600 eV. Periodic boundary conditions are employed and at least of 15 Å slab is used on the surface of few layers to eliminate the interaction between consecutive periodic images. The Monkhorst-Pack k -mesh is set to 11×11 ($11 \times 11 \times 4$) in the Brillouin zone for the self-consistent calculation of few layer cases (bulk), and all atoms are relaxed in each optimization cycle until atomic forces on each atom are smaller than 0.01 eV/Å. As it is well-known that GGA functional underestimates the band gap, all the band structures are computed by using hybrid Heyd-Scuseria-Ernzerhof (HSE06)⁶ functional and the GGA-relaxed crystal structure. It should be noted here that we did not include any effect of exciton binding energy in our DFT calculations to estimate the optical band gap. Biaxial strain is simulated by changing the lattice constant a , whereas the space group

I4/mmm is fixed. The symmetric structure represents the equilibrium positions of the atoms at a given strain value. The distorted structure is obtained by diagonally displacing both the Bi and the Se atoms, but in opposite directions from their equilibrium positions. In what follows, if \mathbf{R}_{Bi} , and \mathbf{R}_{Se} are the equilibrium planer positions of the Bi and Se atoms respectively in a symmetric structure, then in the distorted structure, they assume positions at $\mathbf{R}_{\text{Bi}} + \boldsymbol{\delta}$, and $\mathbf{R}_{\text{Se}} - \boldsymbol{\delta}$, respectively. The outermost Se layers are passivated with hydrogen atoms in order to balance the non-stoichiometry due to the additional Se layer.

Table S1. Elemental compositions as obtained from EDX analysis.

Element	Wt %	At %
O	6.18	40.8
Bi	79.66	40.26
Se	14.16	18.94
Total	100	100

Table S2. Elemental compositions as obtained from ICP-AES measurement.

Element	Wt %	At %
Bi	139.5 mg/lit	66
Se	23.81 mg/lit	31

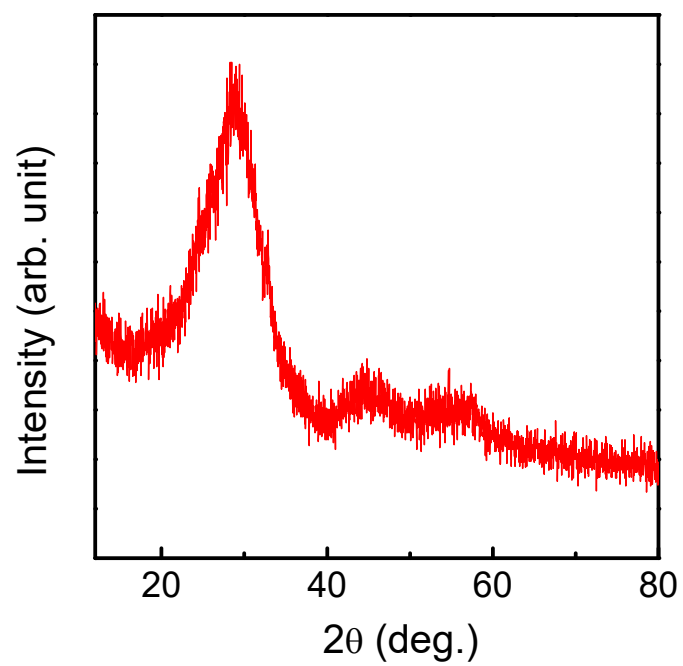


Figure S1. Room temperature XRD pattern of the as synthesized $\text{Bi}_2\text{O}_2\text{Se}$ nanosheets.

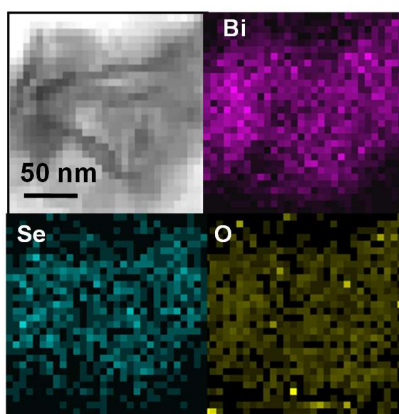


Figure S2. Elemental color mapping exhibiting a homogeneous distribution of Bi, O and Se in the Bi₂O₂Se nanosheet.

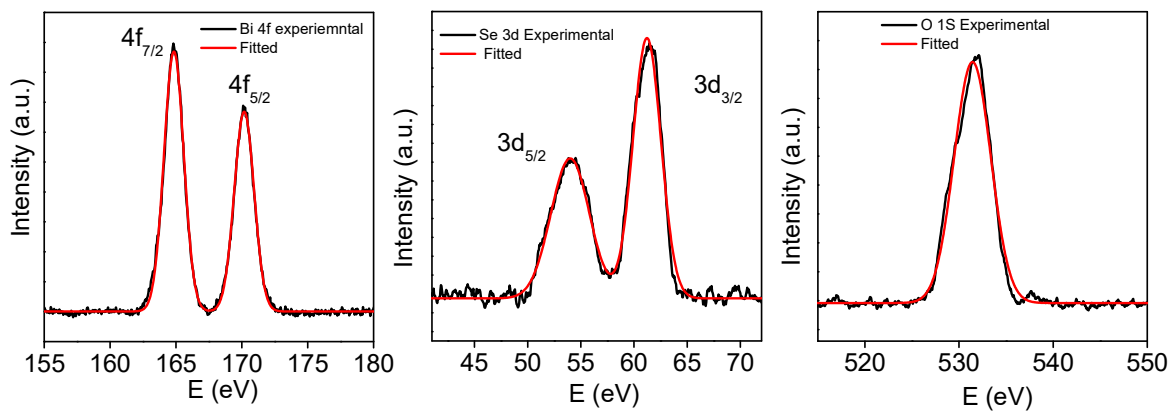


Figure S3. X-ray photoelectron spectra of $\text{Bi}_2\text{O}_2\text{Se}$ nanosheet showing the Bi 4f, Se 3d and O 1s peaks.

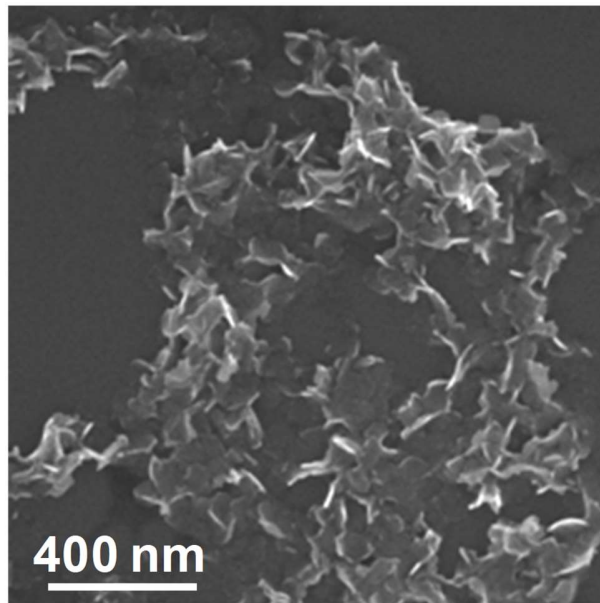


Figure S4. FESEM image of the $\text{Bi}_2\text{O}_2\text{Se}$ nanosheets confirming the sheet like morphology.

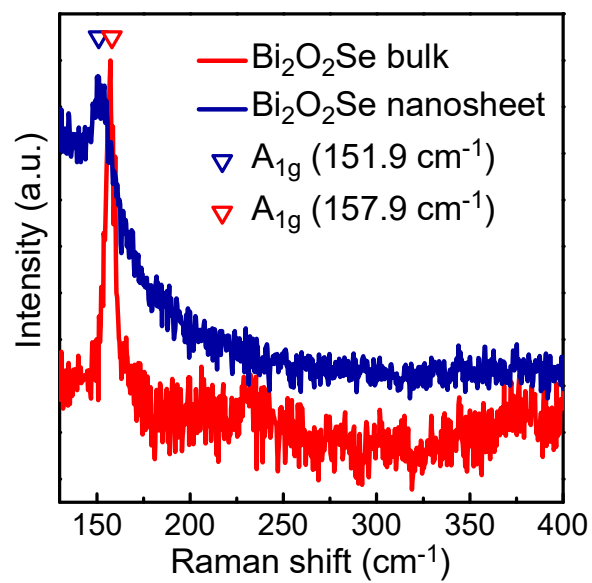


Figure S5. Room temperature Raman spectra of Bi₂O₂Se bulk and nanosheet.

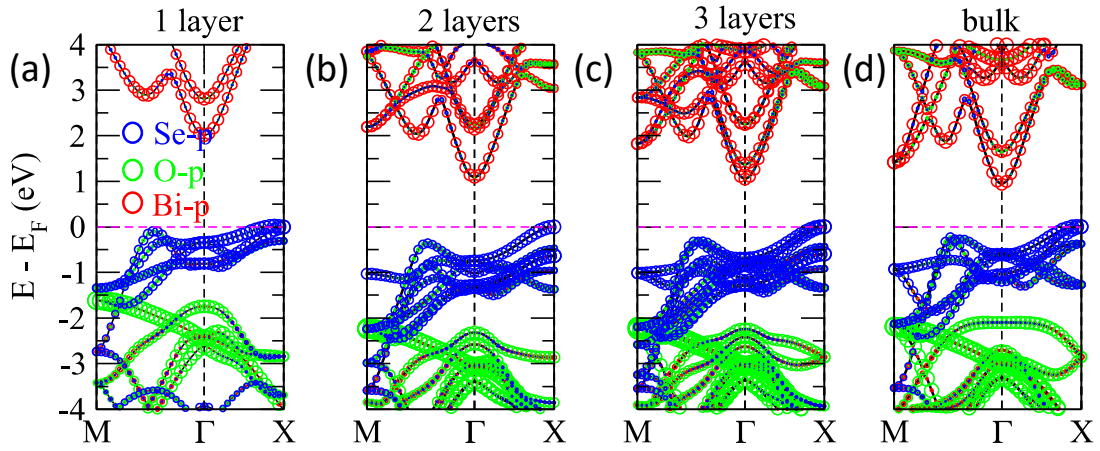


Figure S6. Thickness-dependent and orbital-decomposed band structure of (a) monolayer, (b) bilayer, (c) trilayer and (d) bulk $\text{Bi}_2\text{O}_2\text{Se}$, respectively. Red, green and blue circles indicate the fat-band structure, respectively, for Bi-p, O-p and Se-p orbitals. Magenta dashed line indicates the Fermi level.

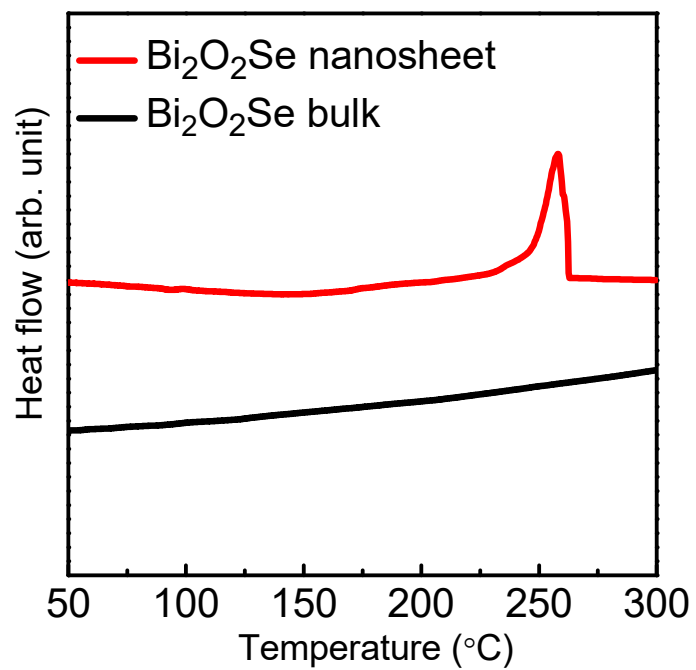


Figure S7. DSC signal of Bi₂O₂Se bulk and nanosheet samples. While the nanosheet sample shows the transition, the bulk does not.

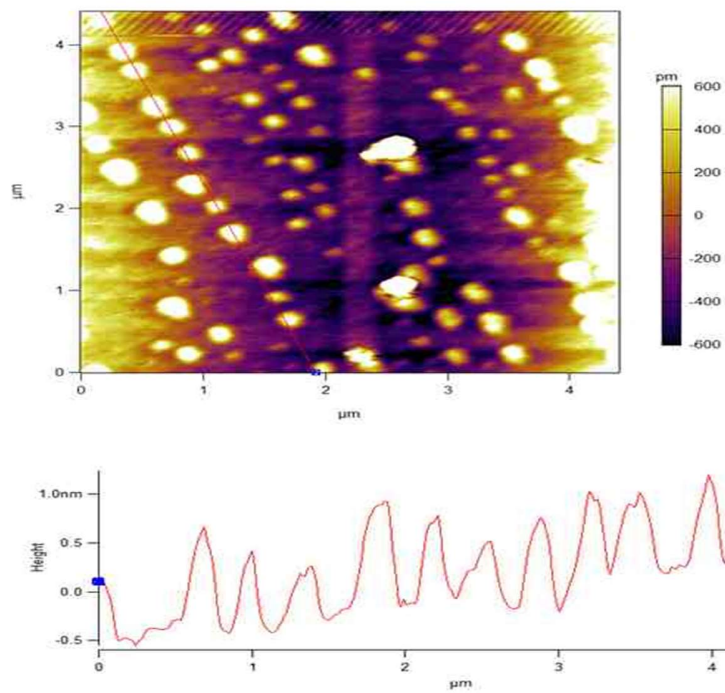


Figure S8. Topography showing 4.5 μm x 4.5 μm area used for PFM measurement.

References

1. Jesse, S.; Baddorf, A. P.; Kalinin, S. V. Switching spectroscopy piezoresponse force microscopy of ferroelectric materials. *Appl. Phys. Lett.* **2006**, *88*, 062908.
2. Jesse, S.; Mirman, B.; Kalinin, S. V. Resonance enhancement in piezoresponse force microscopy: Mapping electromechanical activity, contact stiffness, and Q factor. *Appl. Phys. Lett.* **2006**, *89*, 022906.
3. Perdew, J. P.; Burke, K.; Ernzerhof, M. Generalized Gradient Approximation Made Simple. *Phys. Rev. Lett.* **1996**, *77*, 3865–3868.
4. Kresse, G.; Furthmüller, J. Efficient iterative schemes for *ab initio* total-energy calculations using a plane-wave basis set. *Phys. Rev. B* **1996**, *54*, 11169–11186.
5. Kresse, G.; Joubert, D. From ultrasoft pseudopotentials to the projector augmented-wave method. *Phys. Rev. B* **1999**, *59*, 1758–1775.
6. Heyd, J.; Scuseria, G. E.; Ernzerhof, M. Hybrid functionals based on a screened Coulomb potential. *J. Chem. Phys.* **2003**, *118*, 8207–8215.